Numerical Approach Toward Calculation of Vibration Characteristics of the Multi Axles Truck Using Lagrange Method

Ali Rahmani[1], Ali Mirmohammadi[1], Seyed Mohammad Javad Zeidi [1*], Saeed Shojaei[1]
[1]Shahid Rajaee Training Teacher University
[*]Email of Corresponding Author: smj.zeidi@srttu.edu
Received: July 6, 2015; Accepted: September 14, 2015

Abstract
Initially, the first aim of the present study is to model 3-axle rigid truck by developing a code in Matlab. Secondly, each equation should be drived by acquisition of Lagrange approach. After deriving equations successfully, validation is performed by some result which was mentioned in Bohao Li's master thesis. Although the present approach is totally different from the approach that Boahao Li used in his analysis but the deviation of the present results from that thesis on average is 7 percent which shows an acceptable accuracy in our current numerical approach. In the present study 19 degree of freedoms is used for determining natural frequency and dominant motions. By having dominant motion, it is possible to clarify which region is in endangering of resonance. This paper presents a portion of the results that have been gathered and for watching new result in this field, it is recommended to read our future papers. Solidworks CAD software is also used to calculate mass properties of several components that used in our present study.

Keywords
Natural frequencies, Mode shapes, Lagrange method, Multi-axles truck.

1. Introduction

Generally, vibration analysis includes two kinds of vibration, free and forced vibrations that each one has special principle for determining natural frequency and mode shape. Two main methods are used to extract natural frequency and mode shape in damped forced vibration, the first method is in time domain which uses mode transfer matrix and convolution matrix, in this method modal decomposition is applied to multi DoF systems [1-4]. It should be mentioned that there is little difference between the undamped and damped natural frequencies, and undamped natural frequencies are commonly used to characterize the system [5]. There are many approaches to extract natural frequency that each of them has its advantages and disadvantages, for example Prony method, generalized pencil-of-function method, matrix pencil method, higher order tensor-based method and Newton method [6-13].

The prime aim of this study is to derive the equations of motion by applying the Lagrange method and then base on these equations, natural frequencies can be determined. These natural frequencies can be distinguished for each critical degree of freedom by determining maximum mode shape.

2. Governing Equation

2.1 Calculation of Motion Equation by Acquisition of Lagrangian Approach

Figure 1 illustrates the vibration model of three axles truck, several displacement and mass can be seen in this figure. M1, M2 and M3 are three axles of sample truck. Blue springs are on behalf of tires, red springs show leaf spring which works as the suspension system of this truck, and finally, green springs are utilized to connect chassis and cabin or it can be called cab suspension. W shows displacement, theta shows roll and phi is symbol of pitch during dynamic analysis.

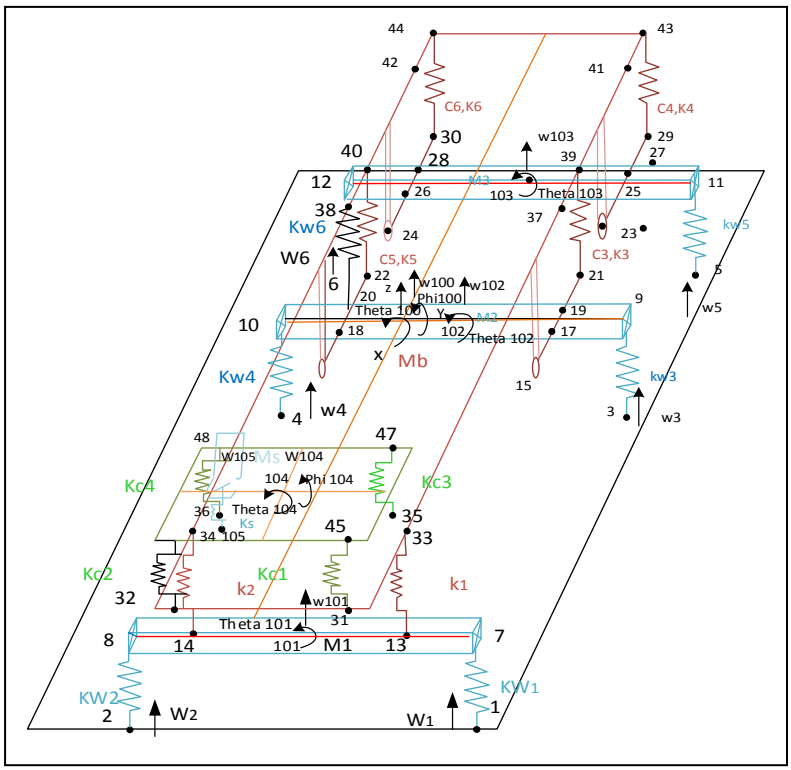

Figure 1. Configuration of 19 DOF for empty truck

Sample truck model is located on a 6-channel excitation rig, so based on this matter vibration system of truck is made of 19 degree of freedom. The 19 DoF are as follow:

- Driver seat bounce
- Cab bounce, pitch and roll
- Chassis bounce (sprung mass), pitch and roll
- Steer axle unsprung mass bounce and roll
- Center axle unsprung mass bounce and roll
- Rear axle unsprung mass bounce and roll
- 6 bounce motion of the 6-channel poster type excitation rig

Motion vector can be written as follow:

$$W_{19} = [w_{106} \quad w_{104} \quad \theta_{104} \quad \varphi_{104} \quad w_{100} \quad \theta_{100} \quad \varphi_{100} \quad w_{101} \quad \theta_{101} \quad w_{102} \quad \theta_{102} \quad w_{103} \quad \theta_{103} \quad w_1 \quad w_2 \quad w_3 \quad w_4 \quad w_5 \quad w_6]^T \tag{1}$$

Where:

W_{19} - Motion degree of 19 DoF truck-poster system model

w_{106} - Deriver seat bounce

w_{104} - Cab bounce
θ_{104} - Cab roll
φ_{104} - Cab pitch
w_{100} - Chassis bounce
θ_{100} - Chassis roll
φ_{100} - Chassis pitch
w_{101} - Steer axle bounce
θ_{101} - Steer axle roll
w_{102} - Center axle bounce
θ_{102} - Center axle roll
w_{103} - Rear axle bounce
θ_{103} - Rear axle roll
w_1 - Bounce of left steer wheel poster type excitation rig
w_2 - Bounce of right steer wheel poster type excitation rig
w_3 - Bounce of left center steer wheel poster type excitation rig
w_4 - Bounce of right center steer wheel poster type excitation rig
w_5 - Bounce of left rear steer wheel poster type excitation rig
w_6 - Bounce of right rear steer wheel poster type excitation rig

3. Calculation of motion equation

The Lagrange's equation can be written as below:

$$\frac{d}{dt}\left(\frac{dT}{d\dot{W}_{19}}\right) - \left(\frac{dT}{dW_{19}}\right) + \left(\frac{dP}{dW_{19}}\right) = 0 \tag{2}$$

Where T is system kinematic energy, P is system potential energy. "W_{19}" is the degree of freedom under generalized coordinate system.
By acquisition of 19 DoF rigid truck-poster vibration system, the system kinematic energy is as follow:

$$\begin{aligned} T = {} & \frac{1}{2}M_s(W`106)^2 + \frac{1}{2}M_c(W`104)^2 + \frac{1}{2}M_b(W`100)^2 + \frac{1}{2}M_1(W`101)^2 + \frac{1}{2}M_2(W`102)^2 \\ & + \frac{1}{2}M_3(W`103)^2 + \frac{1}{2}I_{cx}(\theta`104)^2 + \frac{1}{2}I_{bx}(\theta`100)^2 + \frac{1}{2}I_{1x}(\theta`101)^2 \\ & + \frac{1}{2}I_{2x}(\theta`102)^2 + \frac{1}{2}I_{3x}(\theta`103)^2 + \frac{1}{2}I_{cy}(\theta`104)^2 + \frac{1}{2}I_{by}(\theta`100)^2 \end{aligned} \tag{3}$$

And the system potential energy is as below:

(4)

$$P = \frac{1}{2}K_s(W$$

After deriving each term of equation (2), the terms can be re-arranged as follow:

$$M_{19}W''_{19} + K_{19}W_{19} = 0 \quad (5)$$

M_{19}: System mass matrix of the 19 DoF truck-poster system model
K_{19}: System stiffness matrix of the 19 DoF truck-poster system model
W''_{19}: Acceleration vector of the 19 DoF truck-poster system model
W_{19}: Displacement vector of the 19 DoF truck-poster system model
The last step of deriving equation is calculating mass and stiffness matrixes for 19 DoF system; mass matrix is diametrical, while stiffness matric is not diametrical.

4. Validation of the Numerical Model

The only available data that can be used for validating this numerical model is static deflection which is compared by data of Bohao Li [14]. Although the calculation procedure which was used in this research is different from the procedure of Bohao Li, but both of these methods have similar scope.

As table 1 shows, the results deviation from master thesis of Bohao Li is between 0 to 13 percent which is in average 7 percent. Consequently, this deviation is acceptable for the current numerical approach.

Table1. Static deflection for critical components

	Static Deflection
Seat	-0.0616 (4.19%)
Cab, left front	-0.0088(2.2%)
Cab, right front	-0.0212(1.85%)
Cab, left rear	0.0092(12.2%)
Cab, right rear	-0.0216(1.8%)
Main, steer left	-0.0851(3.8%)
Main, steer right	-0.0871(2.6%)
Main, center left	-0.0374(8.3%)
Main, center right	-0.0405(4.2%)
Main, rear left	-0.0150(14.7)
Main, rear right	-0.0182(18.7%)
Tire, steer left	-0.0159(2.5%)
Tire, steer right	-0.0160(1.8%)
Tire, center left	-0.0095(9.47%)
Tire, center right	-0.0098(12.2%)
Tire, rear left	-0.0040(13.04%)
Tire, rear right	-0.0043(12.24%)

5. Results and Discussion

Table 2 shows natural frequencies, absolute values of mode shapes and dominant motions can be observed for each of 19 DoF model of truck. In each row of this table absolute value of natural frequency and dominant motion which has correlation with that natural frequency are included. As a whole, matrix of mode shape is 19×19 and the biggest mode shape in each column relates the value of each special natural frequency. Dominant motion shows that, in this part of dynamic system, resonance can be observed via this mode shape.

Table 2. Natural frequency, mode shape and dominant motion

Natural frequency(rad/s)	Mode shape(absolute value)	Dominant motion
0.000004622358	0.021047311227522	right rear steer wheel bounce
0.000003451677	**0.020259374677071**	**right steer wheel bounce**
0.000000001065513	0.011408187725685	left rear steer wheel bounce
0.011396794116965	**0.083395256639039**	**Deriver seat bounce**
0.022510398030284	0.076550733036581	Cab roll
0.032668119888841	**0.039167086647959**	**Cab bounce**
50.670520926536	0.027971708759301	right rear steer wheel bounce
51.637956185048	**0.027519431824398**	**left center steer wheel bounce**
64.379923963352	0.032291112815147	left center steer wheel bounce
66.626459703922	**0.099052830331884**	**Cab roll**
70.244931281563	0.060593089737119	Left steer wheel bounce
77.136046229719	**0.053833283682051**	**Right steer wheel bounce**
103.358018471211	0.028267114281256	Rear axle

		bounce
189.294739253455	**0.048448420745559**	**Center axle roll**
189.588958526633	0.048383377462867	Center axle roll
265.249162539134	**0.040630296496336**	**Center axle bounce**
586.273194921182	0.034262703326700	Steer axle bounce
596.770119450067	**0.102992746345498**	**Steer axle roll**
1133.920811119840	0.037746808823452	Steer axle bounce

5. Conclusions

19 DoF truck has been chosen in order to clarify some dynamic characteristic of three axle truck. Mass matrix and stiffness matrices are19×19. Lagrange's approach is used for deriving motion equations. Validation performed by Bohao Li master thesis and there were permissible discrepancies between current numerical method and Bohao Li numerical method. Finally, by utilizing Lagrange equation; natural frequency, mode shape and dominant motion has been calculated. In each separate natural frequency 19 mode shape were available; the biggest mode shape shows the dominant motion, by discerning dominant motion clarifying the region that is critical for occurrence of resonance is possible.

6. Nomenclatures

M_s Mass of seat and deriver, kg

M_c Mass of cab, kg

I_{cx} Inertia of the cab around X axis (roll), kgm^2

I_{cy} Inertia of the cab around Y axis (pitch), kgm^2

M_b Sprung mass excluding the cab, kg

I_{bx} Inertia of the spring mass excluding the cab (roll), kgm^2

I_{by} Inertia of sprung mass ecluding the cab (pitch), kgm^2

M_1 Front axle unsprung mass, kg

I_{1x} Inertia of front axle unsprung mass (roll), kgm^2

M_2 Center axle unsprung mass, kg

I_{2x} Inertia of center axle unsprung mass (roll), kgm^2

M_3 Rear axle unsprung mass, kg

I_{3x} Inertia of center axle unsprung mass (roll), kgm^2

k_s Seat spring stiffness, N/m

k_{c1}, k_{c2}, k_{c3}, k_{c4} Cab suspension spring stiffness, N/m

k_1, k_2 Front axle suspension stiffness, N/m

k_3, k_4, k_5, k_6 Drive axle suspension spring stiffness, N/m

k_{w1}, k_{w2} Front tire stiffness, N/m

k_{w3}, k_{w4}, k_{w5}, k_{w6} Drive tire stiffness, N/m

7. References

[1] Tse, F.S., Morse, I.E. and Hinkle, R.T. 1976. Mechanical Vibration: Theory and Applications, 2nd ed., Allen and Bacon, Inc., Boston.

[2] Dimarogonas, A.D. 1975. Vibration Engineering, West Publishing Co., Inc., New York.

[3] Meiroritch, L. 1967. Analytical Methods in Vibrations, Macmillan Publishing Co., Inc, New York.

[4] Timoshenko, S., Young, D.H. and Weaver, W. 1974. Vibration Problems in Engineering, 4th ed, John Wiley& Sons, Inc., New York.

[5] Wong, J. Y. 2001. Theory of Ground Vehicles, 3rd ed, John Wiley& Sons, Inc., New York.

[6] Kumaresan, R., Tufts, D.W. and Scharf, L.L. 1984. A prony method for noisy data: Choosing the signal components and selecting the order in exponential signal models, Proc. IEEE, 72, 230–233.

[7] Hua, Y. and Sarkar, T. K. 1989. Generalized pencil-of-function method for extracting poles of an em system from its transient response, IEEE Trans. Antennas Propag., 37, 229–234.

[8] Hua, Y. and Sarkar, T.K. 1990. Matrix pencil method for estimating parameters of exponentially damped/undamped sinusoids in noise, IEEE Trans. Acoust., Speech, Signal Process., 38, 814–824.

[9] Pisarenko, Y. F. 1973. The retrieval of harmonics from a covariance function, Geo. Phys. J. Roy. Astron. Soc., 33, 347–366.

[10] Djermoune, E.H. and Tomczak, M. 2009. Perturbation analysis of subspace based methods in estimating a damped complex exponential, IEEE Trans. Signal Process, 57, 4558–4563.

[11] Boyer, R., Lathauwer, L. and Abed-Meraim, K. 2007. Higher order tensor-based method for delayed exponential fitting, IEEE Trans. Signal Process, 55, 2795–2809.

[12] Boyer, R. and Abed-Meraim, K. 2007. Asymptotic performance for delayed exponential process, IEEE Trans. Signal Process. 55, 3139–3143.

[13] Lee, J.H. and Kim, H.T. 2010. Application of Newton Method to Natural Frequency Estimation, IEEE, 58, 212-214.

[14] Li, B. 2006. 3-D dynamic modeling and simulation of a multi-degree of freedom 3-axle rigid truck with trailing arm bogie suspension, M. Eng. thesis, School of Mechanical, Materials and Mechatronic Engineering, University of Wollongong.